

# **DESIGN OF DC DRIVE FOR A MODULAR TRICYCLE**

*A Project Report*

*submitted by*

**KOGANTI ROHIT**

*in partial fulfilment of the requirements  
for the award of the degree of*

**BACHELOR OF TECHNOLOGY  
&  
MASTER OF TECHNOLOGY**



**DEPARTMENT OF ELECTRICAL ENGINEERING  
INDIAN INSTITUTE OF TECHNOLOGY MADRAS.**

**MAY 2013**



# THESIS CERTIFICATE

This is to certify that the project work titled **DESIGN OF DC DRIVE FOR A MODULAR TRICYCLE**, submitted by **KOGANTI ROHIT**, to the Indian Institute of Technology, Madras, for the award of the degree of **Master of Technology and Bachelor of Technology**, is a bonafide record of the project work done by him under our supervision. The contents of this report, in full or in parts, have not been submitted to any other Institute or University for the award of any degree or diploma.

**Dr.Krishna Vasudevan**  
Professor  
Dept. of Electrical Engineering  
IIT-Madras, 600 036

Place: Chennai

Date: 14th May 2013



## **ACKNOWLEDGEMENTS**

It's tough to summarize in a few words the value of the guidance and mentoring provided at all times by my long time professor and project guide, Dr.Krishna Vasudevan. This, not just during every stage of my project, but from much before that, from my first course in Electrical Machines. All I can say is that I'm eternally grateful to him for everything.

I also owe some of my thanks to my friends and seniors, Jeshma, Raviteja, Ramesh, Lokesh, Humpy and others who have offered me much needed help and advice in dire times. The last few months I spent in lab is easily the best time I spent in college, academically, and it is made a much more wonderful experience because of the friends around me in lab, Zubair, Kashyap, Madhuri, Ashwathi and those mentioned before. A special note to Ms. Jayasudha and Mr. Kodandaraman for all the help and support with the equipment.

Finally, I'd like to thank my parents and my close friends here for bearing with my rants during the highs and lows of the project and for their constant show of support, faith and encouragement.

# **ABSTRACT**

**KEYWORDS:** DC Motor, Modular tricycle, Analog drive.

A modular tricycle is a vehicle used by persons with physical injuries or disabilities. The attempt here is to electrically drive a modular tricycle, earlier developed by Ru-TAG, IIT-Madras, so that it becomes a very big advantage to persons with disabilities for locomotion over mechanically run models of tricycles. To drive this tricycle, an appropriate DC motor is to be chosen and a control system built for it so that the speed of the vehicle can be controlled. The control system is a simple current feedback drive built on analog components to make the drive cheaper. So, the project primarily involves selection of the motor, designing the drive and implementing it in hardware. The motor is finally tested on this drive to gauge its control capabilities.

# TABLE OF CONTENTS

|  |             |
|--|-------------|
| <b>ACKNOWLEDGEMENTS</b>                            | <b>ii</b>   |
| <b>ABSTRACT</b>                                    | <b>iii</b>  |
| <b>List of Tables</b>                              | <b>vi</b>   |
| <b>List of Figures</b>                             | <b>viii</b> |
| <b>ABBREVIATIONS</b>                               | <b>ix</b>   |
| <b>1 Introduction</b>                              | <b>1</b>    |
| 1.1 Electrically Driven Modular Tricycle . . . . . | 1           |
| 1.2 Scope of the Project . . . . .                 | 1           |
| 1.3 Selection of the Motor . . . . .               | 2           |
| 1.4 Organization of the Report . . . . .           | 2           |
| <b>2 Design of DC Motor Drive</b>                  | <b>3</b>    |
| 2.1 Modelling of Elements in the Drive . . . . .   | 3           |
| 2.1.1 Dynamic Modelling of a DC machine . . . . .  | 3           |
| 2.1.2 Converter . . . . .                          | 4           |
| 2.2 DC Drive Closed Loop Operation . . . . .       | 6           |
| 2.2.1 Current Control Loop . . . . .               | 6           |
| 2.3 Transfer Functions of the Subsystems . . . . . | 7           |
| 2.3.1 Current Controller . . . . .                 | 7           |
| 2.3.2 Current Feedback . . . . .                   | 8           |
| 2.3.3 Design of the Controller . . . . .           | 8           |
| <b>3 Calculation of Machine Parameters</b>         | <b>13</b>   |
| 3.1 Armature Resistance . . . . .                  | 13          |
| 3.2 Armature Inductance . . . . .                  | 14          |
| 3.3 Motor EMF Constant . . . . .                   | 14          |

|          |  |           |
|----------|--|-----------|
| 3.4      | Frictional Coefficients . . . . .              | 15        |
| 3.5      | Moment of Inertia . . . . .                    | 17        |
| <b>4</b> | <b>Implementation in Hardware</b>              | <b>20</b> |
| 4.1      | Inverter Module . . . . .                      | 20        |
| 4.1.1    | The H-bridge and MOSFETs . . . . .             | 20        |
| 4.2      | Generation of PWM signals . . . . .            | 23        |
| 4.2.1    | Triangular Wave Generator . . . . .            | 23        |
| 4.2.2    | Delay Circuitry for Protection . . . . .       | 25        |
| 4.3      | PI Controller Block . . . . .                  | 29        |
| 4.4      | Feedback Path and Current Transducer . . . . . | 30        |
| 4.5      | Complete Circuit Diagram and Working . . . . . | 32        |
| 4.6      | Testing and Results . . . . .                  | 33        |
| <b>5</b> | <b>Smmary and Conclusions</b>                  | <b>37</b> |
| <b>A</b> | <b>DC Motor Transfer Function</b>              | <b>38</b> |



## LIST OF TABLES

|     |  |    |
|-----|--|----|
| 2.1 | Different Modes of Operation of the H-bridge Circuit . . . . . | 5  |
| 3.1 | Calculation of Motor Constant . . . . .                        | 15 |
| 3.2 | Calculation of the Frictional Coefficients . . . . .           | 16 |
| 4.1 | Calibration of the current transducer . . . . .                | 31 |

## LIST OF FIGURES

|      |  |    |
|------|--|----|
| 2.1  | Block Diagram of DC Motor . . . . .  | 4  |
| 2.2  | H-bridge Circuit . . . . .   | 5  |
| 2.3  | Complete Block Diagram of DC Motor Drive . . . . .   | 6  |
| 2.4  | PWM pattern developed from simultaion . . . . .  | 7  |
| 2.5  | Current Control Loop . . . . .   | 8  |
| 2.6  | The Simulink model of the Drive . . . . .  | 10 |
| 2.7  | Performance of the drive in simulation . . . . .   | 11 |
| 3.1  | Blocked Rotor Test on the Motor . . . . .  | 14 |
| 3.2  | Plot of $T_e$ vs. $\omega$ . . . . .   | 16 |
| 3.3  | Retardation Tests for Moment of Inertia . . . . .  | 17 |
| 4.1  | Two legs of the inverter module, used as a H-bridge circuit. . . . .   | 21 |
| 4.2  | Typical Connection of an IR2110 . . . . .  | 22 |
| 4.3  | IC HPCL2630 . . . . .  | 22 |
| 4.4  | Output from the hardware implementation of the inverter module. Trace 1 is from the Optocoupler output and Trace 2 is the voltage across a resistive load on the H-bridge. . . . . | 23 |
| 4.5  | Connections in a 555 timer and the output . . . . .  | 24 |
| 4.6  | The PWM in implementation and its inverted duplicate. . . . .  | 24 |
| 4.7  | Delay and dead band between signals . . . . .  | 25 |
| 4.8  | Layout of LS123 and its characteristics . . . . .  | 26 |
| 4.9  | X-OR operation to get A' . . . . .   | 26 |
| 4.10 | Outputs from the Delay Circuitry . . . . .   | 27 |
| 4.11 | Outputs from the delay circuitry after correction . . . . .  | 28 |
| 4.12 | Proportional, Integral and Adder Components through Op-amps . . . . .  | 29 |
| 4.13 | Complete PI controller block . . . . .   | 30 |
| 4.14 | Plot of the transducer characteristics . . . . .   | 31 |
| 4.15 | Complete Circuit Diagram . . . . .   | 32 |
| 4.16 | Results from the high-side devices . . . . .   | 33 |

|   |    |
|---|----|
| 4.17 Results from the low-side devices . . . . .                    | 34 |
| 4.18 Different duty cycles from the PWM and the dead band . . . . . | 35 |
| 4.19 Open Loop Response of the Motor . . . . .                      | 36 |
| A.1 DC motor transfer function . . . . .                            | 38 |

## **ABBREVIATIONS**

|              |                               |
|--------------|-------------------------------|
| <b>RuTAG</b> | Rural Technology Action Group |
| <b>PWM</b>   | Pulse Width Modulation        |
| <b>PCB</b>   | Printed Circuit Board         |
| <b>GCB</b>   | General Circuit Board         |
| <b>PI</b>    | Proportional, Integral        |

# **CHAPTER 1**

## **Introduction**

### **1.1 Electrically Driven Modular Tricycle**

A tricycle is a mechanically run vehicle, used generally by physically disabled persons. A modular tricycle tries to overcome the disadvantages in a typical tricycle. In a typical tricycle, the seat height and the arm length of the handle are generally not adjustable and the lack of any cushioning mechanism also makes riding one of these tricycles very hard. The modular tricycle (developed by the RuTAG, IIT-Madras) strives to overcome these issues by making the seat and handle distance adjustable and also provides cushioning for a comfortable ride.

In this major advancement, there is also an attempt to electrically power this tricycle and make this transportation easier for the users. We are not looking at high speeds, but reasonably low top speeds of 10-15 kmph. Electrically powered wheelchairs exist in the market, but they cost around INR 70k and are not affordable, especially by the lower sections of the society who need it the most. So, the idea was to be able to drive the tricycle electrically and still see that cost is not more than INR 15k. This could be made possible by using a cheaper motor and a locally built motor drive. This project is in attempt of doing that.

### **1.2 Scope of the Project**

This project deals with the DC motor drive of the modular tricycle. It includes motor selection, design of the control and its hardware implementation. The motor has to be chosen first by a criteria. Then, we need to design the controller for the motor in simulink after a dynamic analysis and modeling of the DC machine. Then, we proceed to calculate the machine parameters of the motor to arrive at the specifics of the drive. And finally, we come to the hardware implementation of the drive where we build

from scratch an analog controller. Digital controllers are easy and available, but analog controllers are much cheaper compared to them and since cost-cutting is a very important factor in the project, we go with an analog controller.

### **1.3 Selection of the Motor**

The motor to be used for this tricycle was arrived at after a lot of considerations and consultations. Multiple factors weighed into the selection. Firstly, it was important to choose a cheap motor. So, even if there exists very good DC motors for INR 8-10K, we had to aim at something much cheaper. Secondly, the power of the motor had to be lesser than or equal to 250 watts, because otherwise there would be a necessity for a driving license which we are trying to avoid. but it could not also be lesser because it should be able to drive the tricycle and the person. Thirdly, hub motors are most used for this purpose, but they are not preferred here because, not only are they expensive (INR 8K), but they are also not the most reliable machines in rural areas and rugged roads. After having these considerations and sufficient market research, we zeroed in on a Lucas TVS DC motor that is used as a blower motor for bigger cars. It is rated at 12 V and 24 A and possibly suitable for our purpose. But importantly, it is also very cheap (INR 1800), possibly so because it is a large scale manufactured product. In any case, we proceed to use this motor and design our drive for this.

### **1.4 Organization of the Report**

Chapter 2 deals with the modeling of the DC machine, the design of the control system for the motor and simulation results of this drive in simulink.

Chapter 3 is about calculating the machine parameters of the chosen DC motor, the experiments done on the motor to find these and the results.

Chapter 4 explains in detail the hardware implementation of the drive circuitry designed in the second chapter in the analog domain. It also discusses the tested results.

Chapter 5 presents the conclusion. Scope and suggestions for future work on the project is also briefly mentioned.

## CHAPTER 2

### Design of DC Motor Drive

To control a DC motor is to control the amount of armature current flowing and/or the speed of the motor. To do this, we can either control the armature voltage or the field current. In this project, we deal only with the armature voltage control. But before doing that, we need to model the DC motor to know how the armature voltage affects the current(torque) and speed. We use a converter for this purpose. We derive analytically the transfer functions of various blocks of the machine and also the controller used. Using these 'blocks', we will also simulate the drive in simulink and obtain the control values of the PI controller.

#### 2.1 Modelling of Elements in the Drive

In this section, we model the various elements of the drive including the machine and the converter.

##### 2.1.1 Dynamic Modelling of a DC machine

The DC machine electrically primarily consists of the armature resistance and the back-emf from the rotor. But when we give a pulsated DC supply with a converter, the inductance in the armature also starts to have a significant effect and hence should be involved in the modelling, making it a dynamic model of the DC machine.

The DC machine can be electrically expressed in the following equations:

$$v_a = e + i_a.R_a + L\frac{di_a}{dt} \quad (2.1)$$

$$e = K_m.\omega \quad (2.2)$$

$$T_e - T_l = J\frac{d\omega}{dt} + B.\omega \quad (2.3)$$

$$T_e = K_m.i_a \quad (2.4)$$

where  $v_a$  is the armature voltage,

$e$  is the back-emf,

$R_a$  is the armature resistance,

$L$  is the inductance,

$i_a$  is the armature current,

$\omega$  is the speed in rad/s,

$K_m$  is the back-emf constant,

$J$  is the moment of inertia of the machine,

$T_e$  is electric torque developed by the machine and

$T_l$  is the load torque.

Applying the Laplace transform to the first and the third equation and substituting the second and the fourth in them respectively, we get

$$i_a(s) = \frac{v_a(s) - K_m \cdot \omega(s)}{R_a + sL} \quad (2.5)$$

$$\omega(s) = \frac{K_m \cdot i_a - T_l(s)}{B + sJ} \quad (2.6)$$

From these equations, we can draw the block diagram of the DC motor as follows:

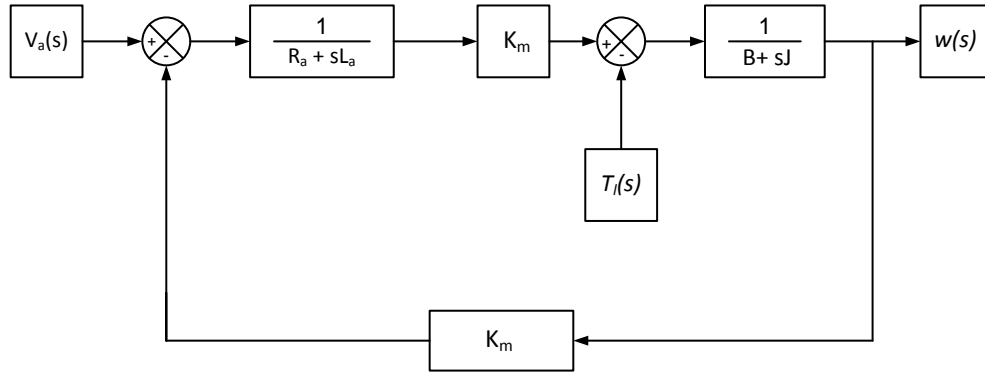


Figure 2.1: Block Diagram of DC Motor

### 2.1.2 Converter

A H-bridge is used as the four-quadrant chopper as shown in Fig 2.2. Each transistor has an anti-parallel diode for the reverse path to the current. There is also a snubber circuit to limit the rate of rise of voltage.



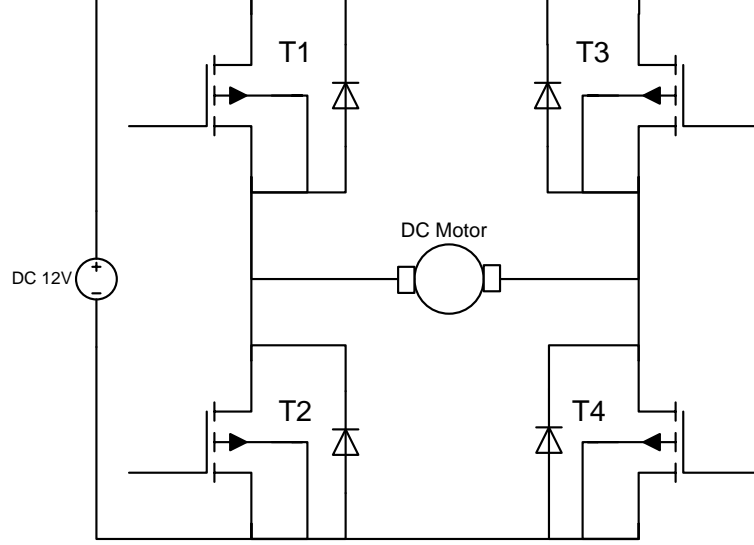


Figure 2.2: H-bridge Circuit

By switching the transistors in different ways, we can achieve various modes of operation of the motor. The various modes are listed in table 2.1.

Table 2.1: Different Modes of Operation of the H-bridge Circuit

| Mode of Operation    | Quadrant | Speed | Torque | $P_{out}$ | $V_a$ | $I_a$ |
|----------------------|----------|-------|--------|-----------|-------|-------|
| Forward Motoring     | 1        | +     | +      | +         | +     | +     |
| Froward Regeneration | 4        | +     | -      | -         | +     | -     |
| Reverse Motoring     | 3        | -     | -      | +         | -     | -     |
| Reverse Regeneration | 2        | -     | +      | -         | -     | +     |

The chopper is modeled as a first-order lag with a gain of  $K_r$ . The time delay corresponds to the statistical average conduction time, which can vary from zero to  $T$ . The transfer function of the converter can then be written as

$$G_r(s) = \frac{K_r}{1 + \frac{sT_r}{2}} \quad (2.7)$$

where  $K_r = V_s/V_c$ ,  $V_s$  is the source voltage, and  $V_c$  is the maximum control voltage. Increasing the chopper frequency decreases the delay time, and hence the transfer function becomes simple gain.

## 2.2 DC Drive Closed Loop Operation

A typical DC drive consists of two loops, an outer speed control loop and an inner current control loop. Inner current loop is also called as the torque control loop as armature current is directly proportional to the torque generated. The outer speed loop is the slower one and the inner loop is faster relatively and makes the control respond better. So we generally use two loops. But in our case, a modular tricycle, the user is expected to take visual feedback of the speed of the vehicle(also from the speedometer) and adjust the speed reference accordingly. So, we design and implement only the inner current control loop for our purposes. The overall block diagram of the DC drive with the speed control loop is as shown in the fig 2.3.

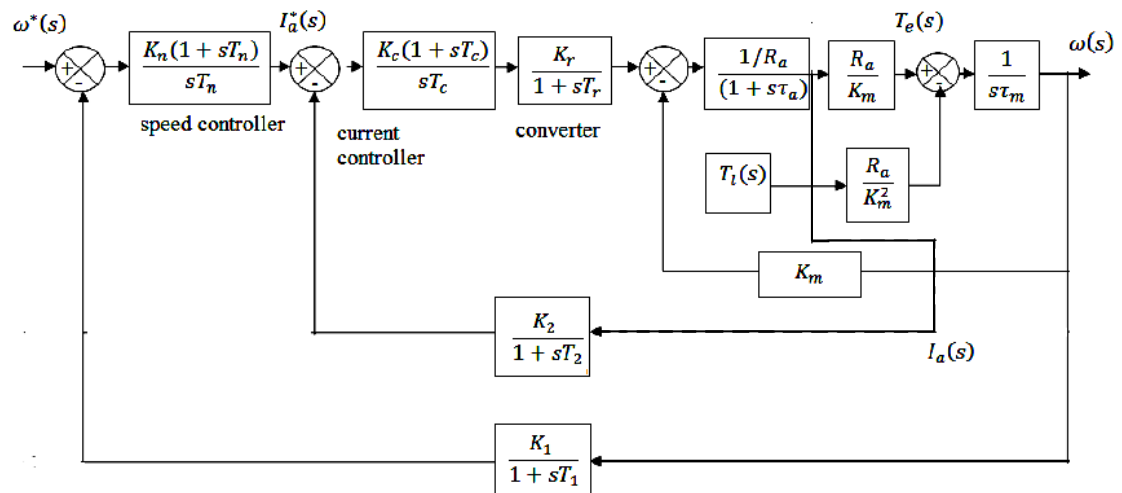


Figure 2.3: Complete Block Diagram of DC Motor Drive

The control loop(s) of the DC motor works in the following way. When a current reference is given to the loop, it is compared with the present value of the current and the error is processed through the current controller. The output of the current controller then decides the base drive signals of the chopper circuit.

### 2.2.1 Current Control Loop

With the inner current control loop alone, the motor drive is a torque amplifier. The current controller can either be a PWM controller or a Hysteresis controller. In this design, we use the PWM controller.

The current error is fed into a controller, generally PI. Current error is amplified through this controller and emerges as a control voltage. It is required to generate a proportional armature voltage from the fixed voltage source by appropriate switching of the devices in the H-bridge circuit. Its realization is as follows. The control voltage is compared with a triangular wave to generate the ON and OFF times. ON signal is produced if the control voltage is greater than the triangular (carrier) wave; OFF signal is generated when the control signal is less than the carrier signal. The PWM switching pattern can be seen in figure 2.4. When it is logic one, switches T1 and T4 are switched on and when it is logic zero, T2 and T3 are switched on and T1 and T4 are switched off.

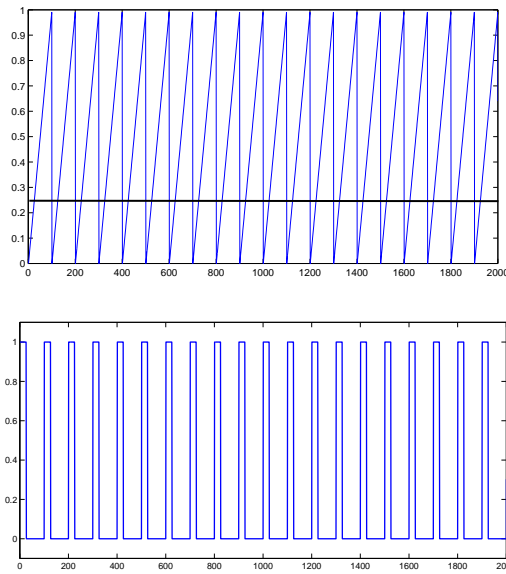


Figure 2.4: PWM pattern developed from simulation

## 2.3 Transfer Functions of the Subsystems

### 2.3.1 Current Controller

The current controller is of the proportional integral type. It can be represented as the following transfer function:

$$G_c(s) = K_p + \frac{K_i}{s} \quad (2.8)$$

where  $K_p$  and  $K_i$  are the gain constants of the controller.

### 2.3.2 Current Feedback

The gain of the current feedback is  $K$ . We are using a low-pass filter to filter ripple in the current before feeding back to the controller. Generally time constant of the filter might not be greater than a millisecond. The transfer function of the current filter is

$$H(s) = \frac{K}{1 + sT} \quad (2.9)$$

where  $K$  is the gain and  $T$  is the time constant.

### 2.3.3 Design of the Controller

#### Block Diagram of Inner Loop

Using the transfer functions of the PI controller, the converter, the feedback filter, the current controller loop is shown as a block diagram below. The third block- transfer function can be arrived at easily and is explained in the appendix.

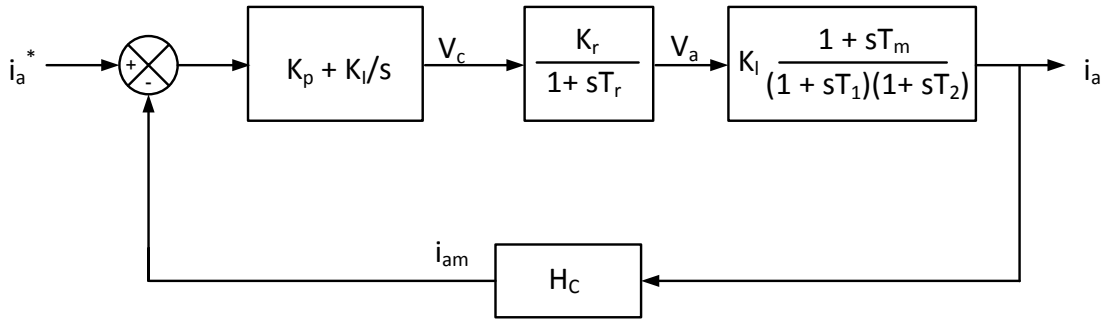


Figure 2.5: Current Control Loop

#### $K_i, K_p$ values through Simulation

Using the transfer functions arrived at and the block diagram from them, we simulate the behavior of the drive circuit to determine the optimal values for  $K_i$  and  $K_p$ . The simulation is done in MATLAB Simulink. But to test the driver circuit of the motor, we need to plug in the parameters of the particular motor we are using. We derive the parameters of the chosen motor using methods described in Chapter 3 and arrive at the

following values of motor constants:

$$R_a = 0.1789 \, \Omega, \quad (2.10)$$

$$L = 300 \, \mu H, \quad (2.11)$$

$$J = 0.000318616 \, kg.m^2, \quad (2.12)$$

$$K_m = 0.021374 \, V/rad/s, \quad (2.13)$$

$$B = 9 \times 10^{-5} \, Nm/rad/s \quad (2.14)$$

We will also see in Chapter 3 that for this particular motor,  $T_e$  and  $\omega$  don't have a linear relationship but in fact a second order functionality. There is therefore a second degree friction coefficient  $B'$  whose value is found to be

$$B' = 2.1 \times 10^{-6} \, Nm/(rad/s)^2 \quad (2.15)$$

The next figure 2.6 shows the simulink model used, followed by the results. After many iterations,  $K_p$  and  $K_I$  values are found to be 10 and 3 respectively. The top window in fig 2.7 shows the load on the motor and its variation with time. We see that the speed in the second window also adjust accordingly with the load, once at  $t = 2 \, secs$  and again at  $t = 5 \, secs$  more so since the armature current, as seen in the third window, is fed back to keep it constant at the reference value of 18A.

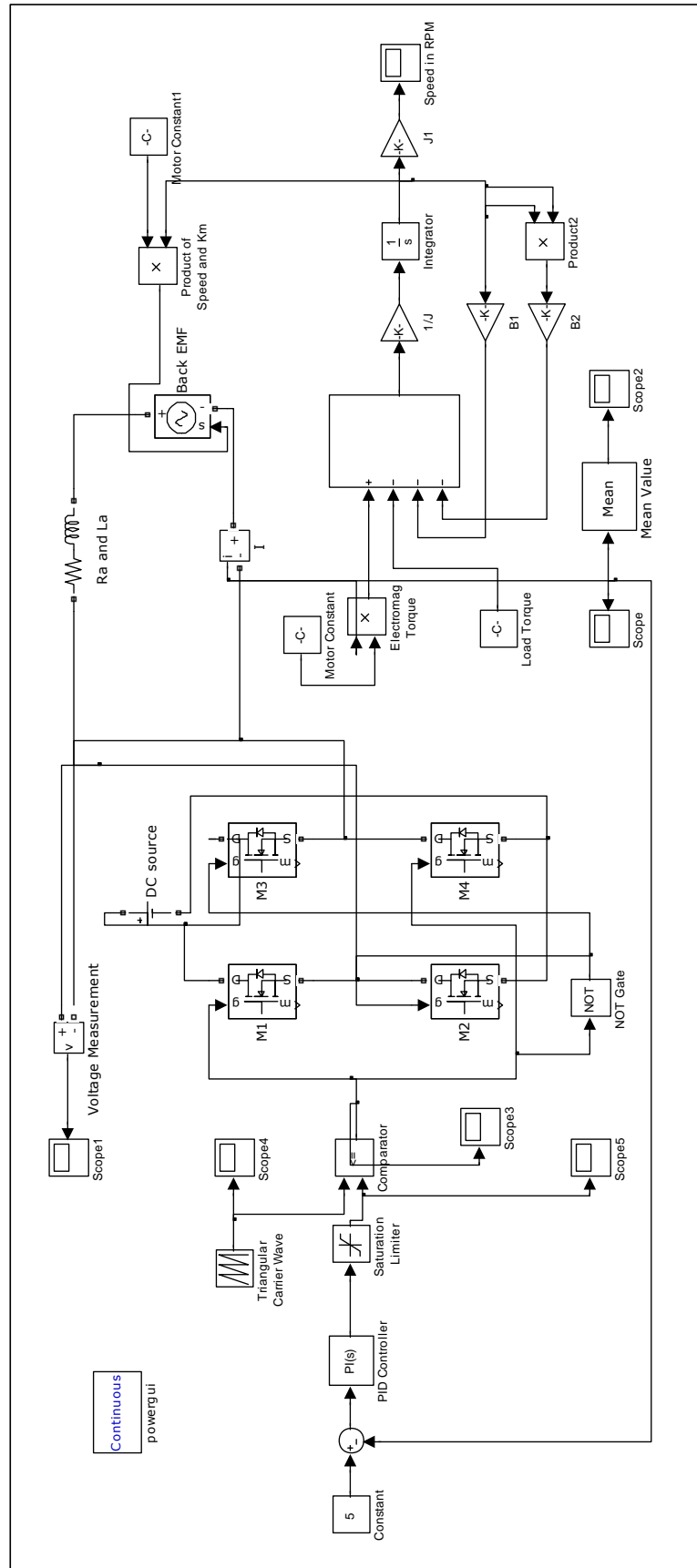


Figure 2.6: The Simulink model of the Drive

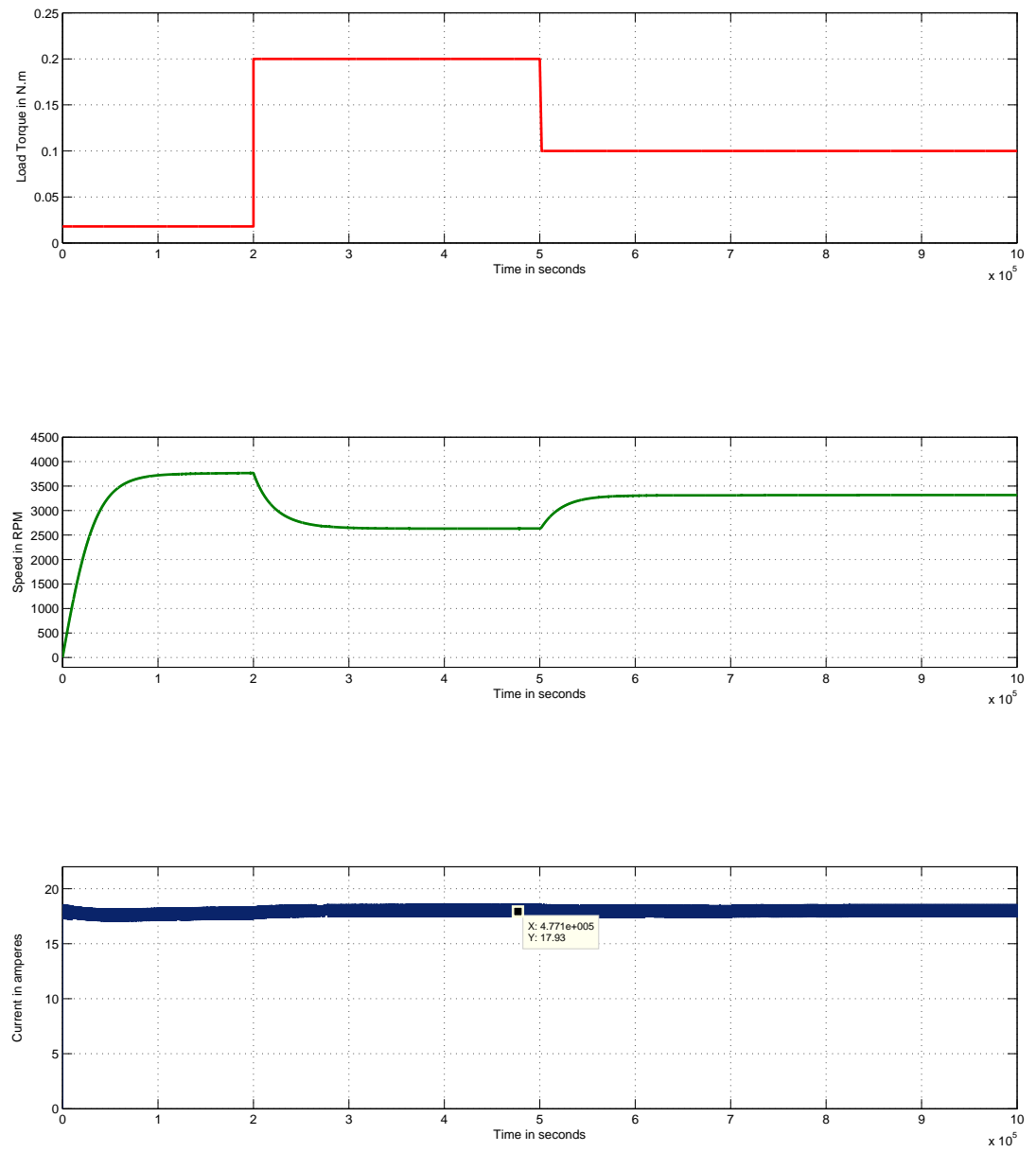


Figure 2.7: Performance of the drive in simulation





## CHAPTER 3

### Calculation of Machine Parameters

The essential characteristics of any controller depends very much on the machine parameters. This chapter deals with the calculation of those parameters through experiments on the machine. The important machine parameters we will calculate are armature resistance, armature inductance, motor constant, moment of inertia and friction coefficients. The ratings of the DC motor we are trying to find the parameters for is rated at 12 V and 24 A.

#### 3.1 Armature Resistance

To find the armature resistance, a trivial way is to connect an ohm-meter across the armature terminals and find the resistance. But this reading won't be exact because of ohm-meter's own internal resistance. An easy way is to block the rotor and apply a small DC voltage at the armature and measure the current. Thereby, we can calculate the resistance by Ohm's law. If the resistance is too small, we can use an external resistance to limit the value of current. This way, we can find the armature resistance. The basic equation is:

$$v_a = i_a \cdot R_a + v_b \quad (3.1)$$

where  $v_b$  is the brush drop.

The plot of  $v_a$  vs  $i_a$  in figure 3.1 has a negative intercept implying there is a negative brush drop but this is not possible. There can't be any armature current for zero  $v_a$ . This means that the graph, for very low values of  $v_a$ , has a very steep slope and  $v_b$  can be safely ignored. The armature resistance is found from the slope to be  $0.1789\Omega$

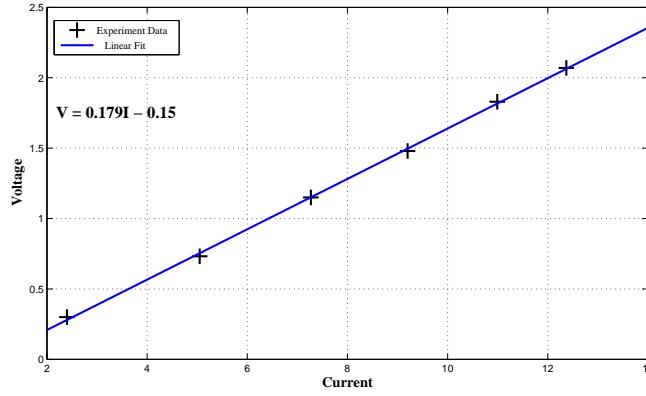


Figure 3.1: Blocked Rotor Test on the Motor

## 3.2 Armature Inductance

The armature inductance is important for the dynamic model of a DC machine. There are experimental ways to find the armature inductance but the easier way out is to use a LCR meter and measure the inductance across the armature terminals. Using an LCR meter, we find the inductance to be 300 mH.

## 3.3 Motor EMF Constant

The operational equation for the motor is given by

$$v_a = i_a \cdot R_a + e \quad (3.2)$$

$$e = K_m \cdot \omega \quad (3.3)$$

The motor is operated at particular speeds, on/off load and this speed is monitored with a tachometer. When a voltage is applied at the armature, and current flows in the circuit, we can estimate from these and the found  $R_a$  ( $0.18\Omega$ ), the back-emf  $e$  of the machine from the above relation. Once back-emf is found, the motor constant  $K_m$  is just the back-emf divided by the speed. We calculate the motor constant this way, from different values of voltage, current and speed. The experimental results are as follows in table 3.1. The averaged motor constant is found to be  $K_m = 0.0214 \text{ V/rad/s}$

Table 3.1: Calculation of Motor Constant

| $v_a$ (volts) | $i_a$ (amps) | $\omega$ (rpm) | $K_m$ (volts/rpm) |
|---------------|--------------|----------------|-------------------|
| 5.00          | 5.475        | 1820           | 0.0022145         |
| 6.00          | 7.058        | 2127           | 0.0022356         |
| 7.00          | 8.842        | 2430           | 0.0022311         |
| 8.00          | 10.777       | 2705           | 0.002244          |
| 9.00          | 12.837       | 2970           | 0.0022667         |

### 3.4 Frictional Coefficients

The frictional forces on a DC machine can have an impact on its operation if the machine is big and should be taken into consideration while modeling a drive for it. The equation of operation here that gives us the coefficients is:

$$J \frac{dw}{dt} = T_e - T_l - B_0 - B_1 \cdot \omega - B_2 \cdot \omega^2 \quad (3.4)$$

The higher order coefficients are usually too small, so we ignore them, including  $B_2$ . Now, we are trying to get  $B_0$  and  $B_1$  from this equation. When the motor is running at a constant speed (not accelerating or decelerating), the LHS of the equation becomes zero. Also, we will run the motor at no load and this makes  $T_l$  zero. Then, we have only the coefficients' terms and the electromagnetic torque  $T_e$  in the equation.

$$T_e = B_0 + B_1 \cdot \omega + B_2 \cdot \omega^2 \quad (3.5)$$

$T_e$  is a product of  $i_a$  and  $K_m$  and so, we can tabulate and plot  $T_e$  vs.  $\omega$ , and we get the results in Fig 3.2.

When we try to fit a curve, a second degree polynomial fits, indicating that even  $B_2$  is non-zero and significant, as we can see from the curve of the graph. We end up with the following values for the coefficients:

$$B_0 = 0.0183 \text{ Nm} \quad (3.6)$$

$$B_1 = 9 \times 10^{-5} \text{ Nm/rad/s} \quad (3.7)$$

$$B_2 = 2 \times 10^{-6} \text{ Nm/(rad/s)}^2 \quad (3.8)$$

Table 3.2: Calculation of the Frictional Coefficients

| $v_a$ (volts) | $i_a$ (amps) | $\omega$ (rad/s) | $T_e$   |
|---------------|--------------|------------------|---------|
| 1.58          | 1.53         | 61.35            | 0.03257 |
| 1.98          | 1.81         | 77.78            | 0.0385  |
| 3.11          | 2.91         | 121.61           | 0.0620  |
| 3.74          | 3.67         | 144.82           | 0.0781  |
| 4.26          | 4.41         | 163.02           | 0.0939  |
| 5.01          | 5.475        | 189.30           | 0.1166  |
| 5.11          | 5.67         | 192.35           | 0.1207  |
| 6.018         | 7.058        | 223.34           | 0.1503  |
| 6.471         | 7.9          | 237.54           | 0.1682  |
| 7.0036        | 8.842        | 254.64           | 0.1883  |
| 7.5765        | 9.922        | 272.47           | 0.2113  |
| 7.9936        | 10.777       | 284.87           | 0.2295  |
| 8.3454        | 11.505       | 295.28           | 0.245   |
| 9.0288        | 12.837       | 316.18           | 0.2733  |

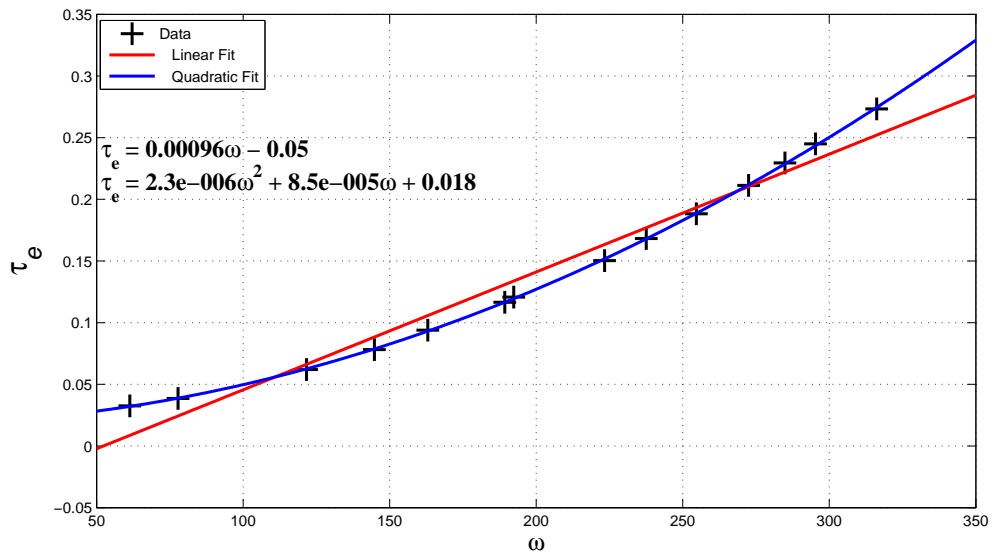


Figure 3.2: Plot of  $T_e$  vs.  $\omega$

### 3.5 Moment of Inertia

The moment of inertia is a very important property of a motor and the drive depends very much on this property. Moment of inertia can be measured by the retardation test. This test works on the principle that when a motor is switched off from a certain speed, all the mechanical energy stored in the motor is dissipated through the frictional forces on the motor. Recalling equation 3.4, this time, when the power is switched off through a mechanical switch (to avoid the capacitive effects of the power source), the electromagnetic torque immediately goes to zero because the current becomes zero instantaneously. The motor is run on no load, so the load torque is also zero. This time, the motor starts decelerating, so the LHS term won't be zero. The equation reduces to:

$$J \frac{dw}{dt} = -B_0 - B_1 \cdot \omega - B_2 \cdot \omega^2 \quad (3.9)$$

For different speeds, we do the retardation test and capture the falling speed vs. time repeatedly. From the plots, we can get the slope, and using the equation, moment of inertia  $J$ . We show here two of the plots in figure 3.3. The plots are for when the motor is switched off from 3180 rpm and 4770 rpm, respectively. The moment of inertia is found and averaged out to be  $3.1861 \times 10^{-4} \text{ kg.m}^2$

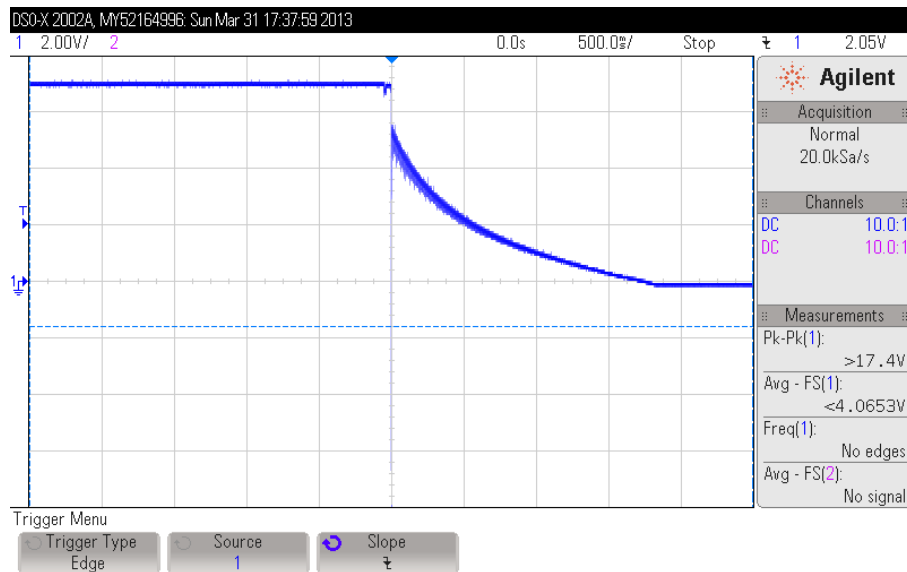
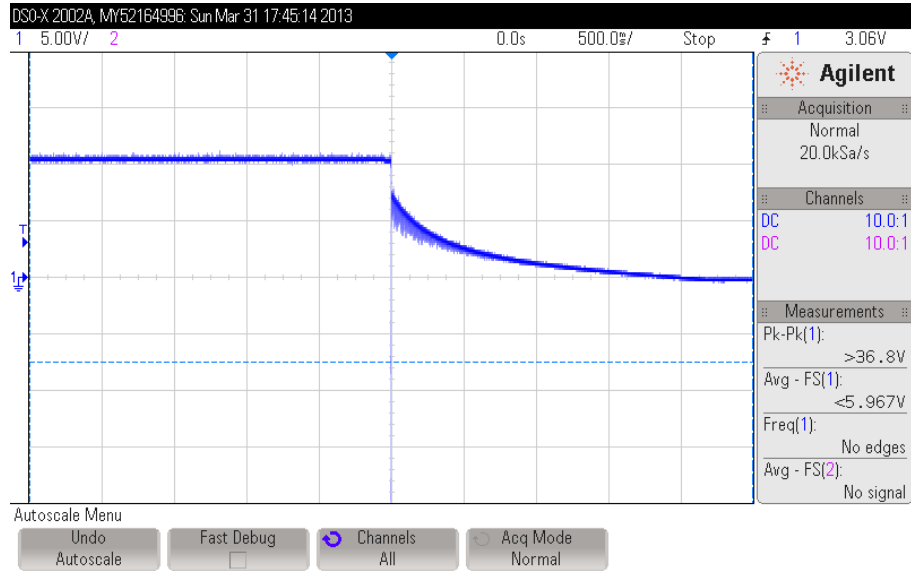


Figure 3.3: Retardation Tests for Moment of Inertia



The machine parameters calculated from all these experiments are as follows:

$$R_a = 0.1789 \, \Omega, \quad (3.10)$$

$$L = 300 \, \mu H, \quad (3.11)$$

$$J = 3.1861 \times 10^{-4} \, kg.m^2, \quad (3.12)$$

$$K_m = 0.021374 \, V/rad/s, \quad (3.13)$$

$$B_0 = 0.0183 \, Nm \quad (3.14)$$

$$B_1 = 9 \times 10^{-5} \, Nm/rad/s \quad (3.15)$$

$$B_2 = 2 \times 10^{-6} \, Nm/(rad/s)^2 \quad (3.16)$$



# CHAPTER 4

## Implementation in Hardware

The implementation in hardware proceeds over various stages and blocks. They are the inverter module, PWM signal generator, PI controller block and the feedback path. All these blocks are wired up on different PCBs/GCBs and tested individually before using them together for the complete functionality of the drive. Each of them are individually explained in this chapter.

### 4.1 Inverter Module

The inverter module contains the H-bridge, the DC bus for it, the driver ICs for the MOSFETs and other protection circuitry. The layout for all these components is developed on a PCB and it is populated with them. The two legs of the inverter has independent circuits and driver ICs arranged in parallel on the PCB. Each component and its application here is explained in brief. The results from the hardware is shown in figure 4.4

#### 4.1.1 The H-bridge and MOSFETs

There are three legs on the inverter PCB and we use only two of them. The four switches that are in the two legs are used in a H-bridge formation with the motor/load to be connected across the H, as in figure 4.1. The choice of suitable switches, MOSFETs here, is also important. The motor is rated at 20A and 12V, so the switch should be able to conduct that. A low voltage drop and resistance across the switch would be an added advantage. With these constraints, we use the MOSFET IRF3205, which can conduct upto 80A and has a low  $R_{ds}$  of  $8.0\text{ m}\Omega$ .

Another problem with the large currents that are characteristic of this motor is the sustainability of the PCB of these currents. To test this, the ground and DC buses are shorted on the PCB and a small voltage is applied ( 3V) to it. It is found that the PCB



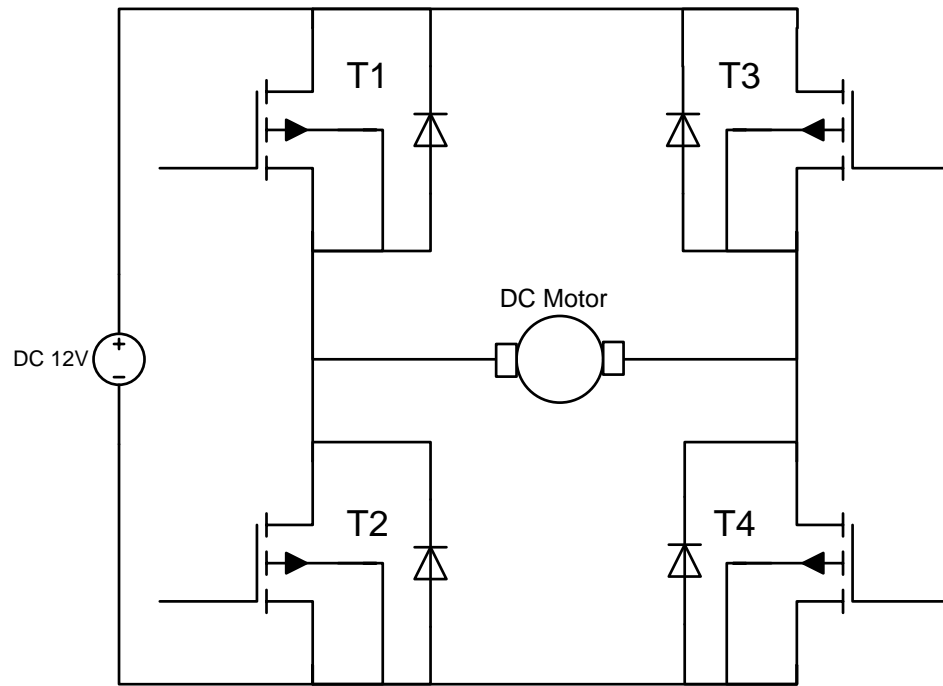


Figure 4.1: Two legs of the inverter module, used as a H-bridge circuit.

can carry upto nearly 18A before the tracks starts getting heated up beyond  $50^{\circ}C$ . So, the MOSFETs are mounted along with sufficient heat sinks on the board and care is taken to make thick interconnections between MOSFETs on the same leg and between the legs (using a thick braided wire) to enable them to carry rated currents.

### IC IR2110

The driving signal to the four MOSFETs comes from the driver ICs IR2110. Each 2110 can drive two MOSFETs. The TTL values (of 3.3-5 V) that we get at the inverter board are not sufficient to drive the MOSFETs. Also, each MOSFET's gate signal should be driven over and above the source and it is not easy, particularly for the High-side FETs. So, the IR2110s are used here as high speed MOSFET drivers with independent high and low side referenced output channels. They can drive 10-20 V at the output. The schematic of the 2110's arrangement is shown in figure 4.2.

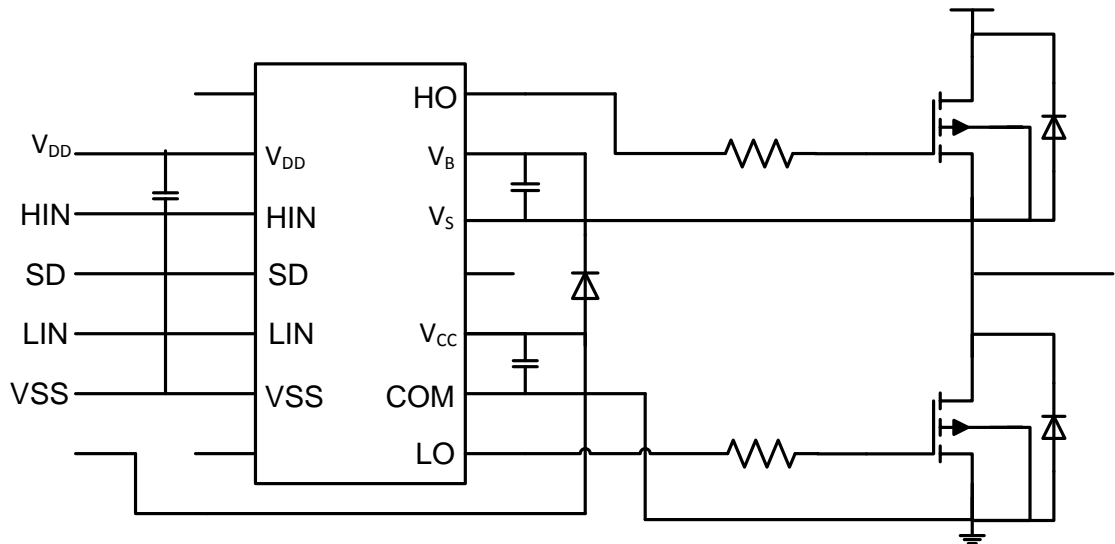


Figure 4.2: Typical Connection of an IR2110

### Opto-coupler IC

The input to the IR-2110 comes from the optocouplers and the inputs to the optocoupler comes from the PWM block. Optocouplers are electronic ICs that transfers electrical signals between isolated parts of the circuit through light. They take electrical input that lights up an LED and the intensity of this is sensed by an isolated photo sensors that drive BJTs. These ICs are for the protection of the circuit from accidental surges at the inputs. One HPCL 2630 IC here has two optocouplers inside and is connected to an IR.

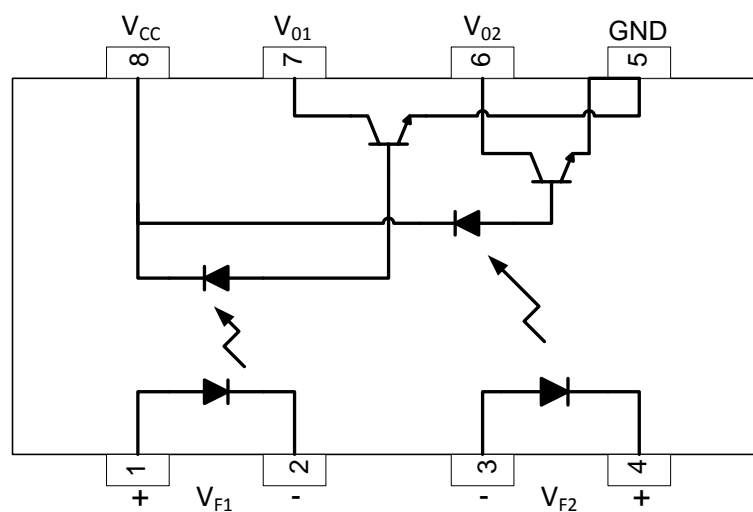


Figure 4.3: IC HPCL2630

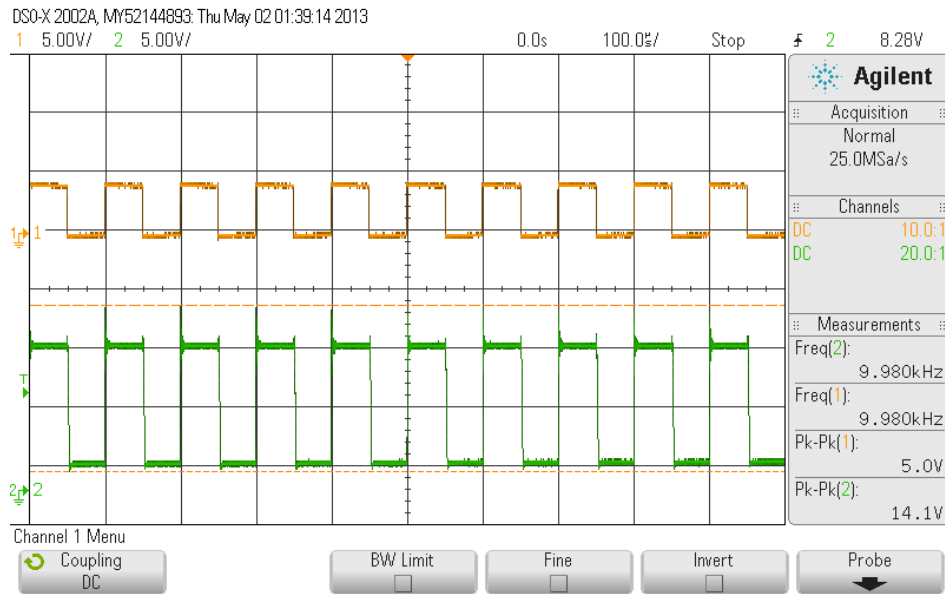


Figure 4.4: Output from the hardware implementation of the inverter module. Trace 1 is from the Optocoupler output and Trace 2 is the voltage across a resistive load on the H-bridge.

## 4.2 Generation of PWM signals

This block, after the PI controller, takes the reference value from it and compares it with a triangular carrier wave generated locally to produce pulse width modulated (PWM) signal with a switching frequency of 10 kHz. This signal is duplicated and inverted and also passed through a delay circuit to avoid shorting the inverter legs. The comparator gives the output peak to peak of 5V and this is also the output voltage of the block.

### 4.2.1 Triangular Wave Generator

To generate a triangular wave of frequency 10 kHz, we use a 555 oscillator. A 555 timer is a common IC used in a number of timer, pulse generation and oscillator applications. The 555 can be used to provide time delays, as an oscillator and as a flip flop element. The 555 has three operating modes, monostable, astable and bistable. Here, we use it in the astable mode as an oscillator. When used in the configuration in figure 4.5, we get a square wave at pin 3. The values of  $R_1$ ,  $R_2$  and  $C$  to be used to get 10 kHz can be got from the adjacent graph. Or simply, the frequency of the square wave in terms of

$R_1$ ,  $R_2$  and  $C$  is given by

$$f = \frac{1.4}{(R_1 + 2R_2) \cdot C} \quad (4.1)$$

From this equation, we choose  $C = 0.01\mu F$ ,  $R_1 = 1k\Omega$ ,  $R_2 = 6.8k\Omega$  to get 10kHz.

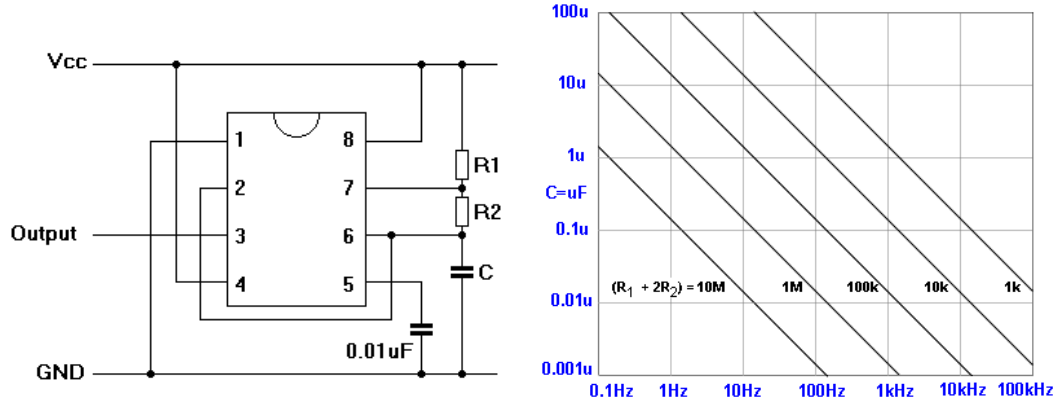


Figure 4.5: Connections in a 555 timer and the output

We get a square wave of 10kHz and to convert it into a triangular wave, we use an RC combination of  $200\Omega$  and  $0.2\mu F$  by charging and discharging the capacitor. The resulting PWM signal is duplicated and inverted through a 4069 NOT gate before both proceed to the delay circuit.

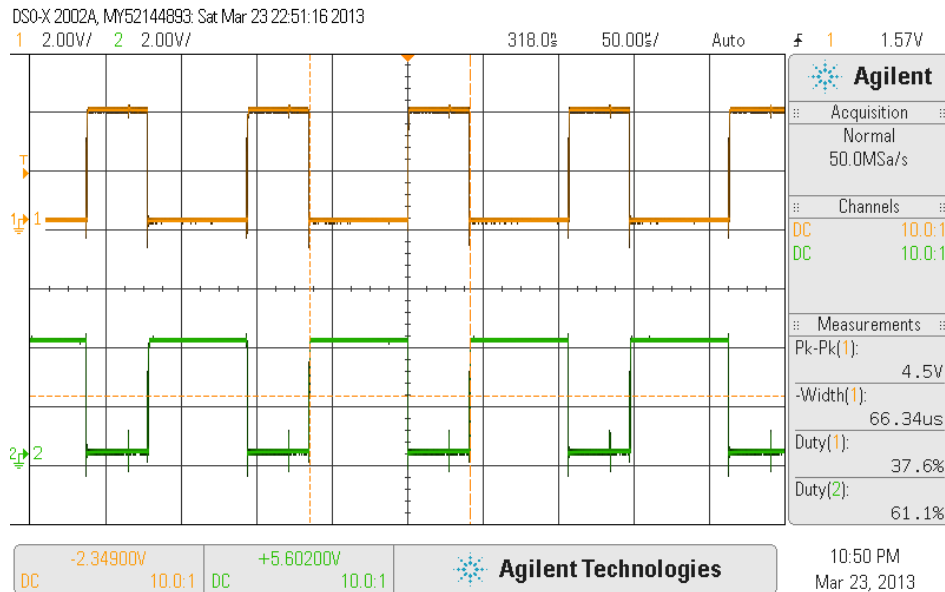


Figure 4.6: The PWM in implementation and its inverted duplicate.

### 4.2.2 Delay Circuitry for Protection

While feeding the gate pulses to the inverter module, we have to take care that no two switches in the same leg are on continuously. If both switches of the same leg are on, then the source voltage will be shorted and huge current will flow and damage the switches. So there should be a blanking period for which both the switches are off. The delay circuit is to provide this blanking period.

Let  $A$  and  $B$  (inverse of  $A$ ) be the PWM signals we need delayed signals  $A'$  and  $B'$  as shown in the Fig 4.7. Then we will give the  $A'$  and  $B'$  signals to drive the top and bottom switches of the same leg. Hence, we'll be able to achieve blanking for the circuit.

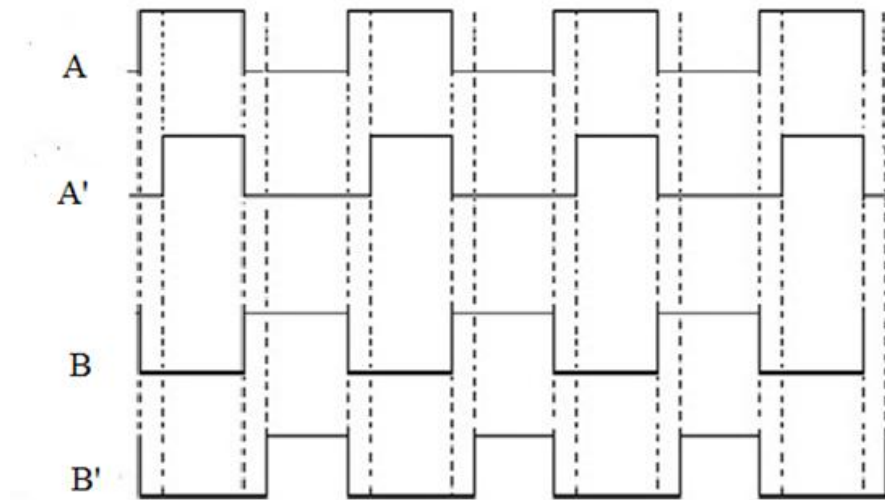


Figure 4.7: Delay and dead band between signals

Now, the objective is to get  $A'$  and  $B'$  from  $A$  and  $B$ . To get that, we use the 74LS123 and 74LS86 ICs:

- In 74LS123, the rising edge is detected and an impulse signal  $Q$  is generated for the required duration. The duration of the impulse is given in the equation 4.2.
- Then, an X-OR operation is performed on the original signal and the impulse generated and what we get is the delayed signal  $A'$  as can be seen in the figure 4.9.
- The same operation is performed on the inverted signal  $B$  and we get the delayed signal  $B'$ . We end up having the two required signals  $A'$  and  $B'$ .

The output pulse duration is essentially determined by the values of the external

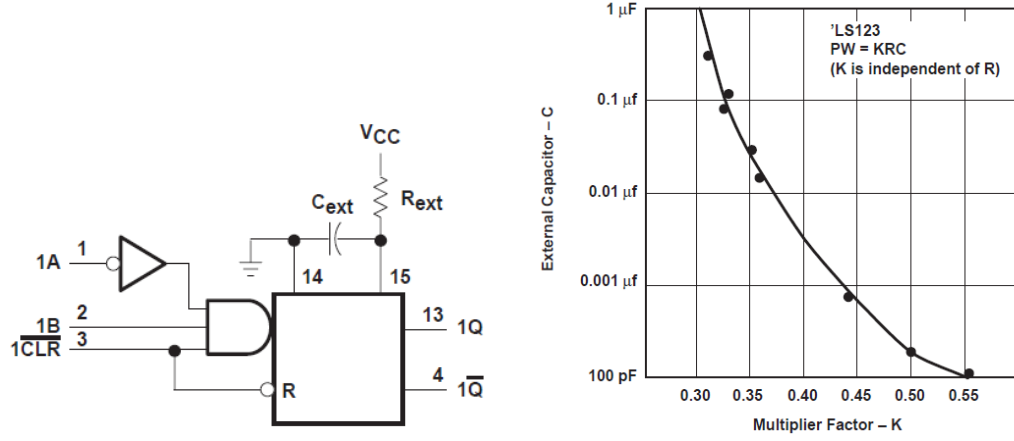


Figure 4.8: Layout of LS123 and its characteristics <sup>1</sup>

capacitance and the timing resistance. For pulse duration when  $C_{ext} < 1\mu F$ , we use the following equation.

$$T_w = K.R_t.C_{ext} \quad (4.2)$$

where  $K$  is the multiplier factor, in this case 0.55,  $R_t$  is in  $k\Omega$  and  $C_{ext}$  is in  $pF$ , while  $T_w$  is in  $ns$ .

We choose  $C_{ext} = 100pF$  and  $R_t = 12k\Omega$ . So, we get a delay of

$$T_w = 0.55 * 12 * 100ns = 660ns \quad (4.3)$$

The delay circuit is thus designed as shown and the X-OR operation of A and Q gives the desired delayed signal A' (Fig 4.9). The results that follow (Fig 4.10) show the output and the two delayed signals that drive the inverter module.

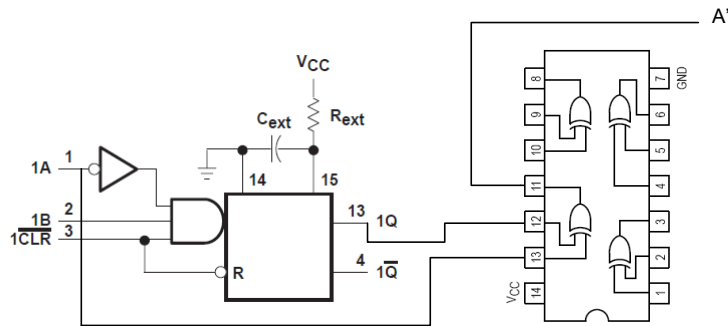


Figure 4.9: X-OR operation to get A'

<sup>1</sup>Taken from <http://www.ti.com/lit/an/sdla006a/sdla006a.pdf>

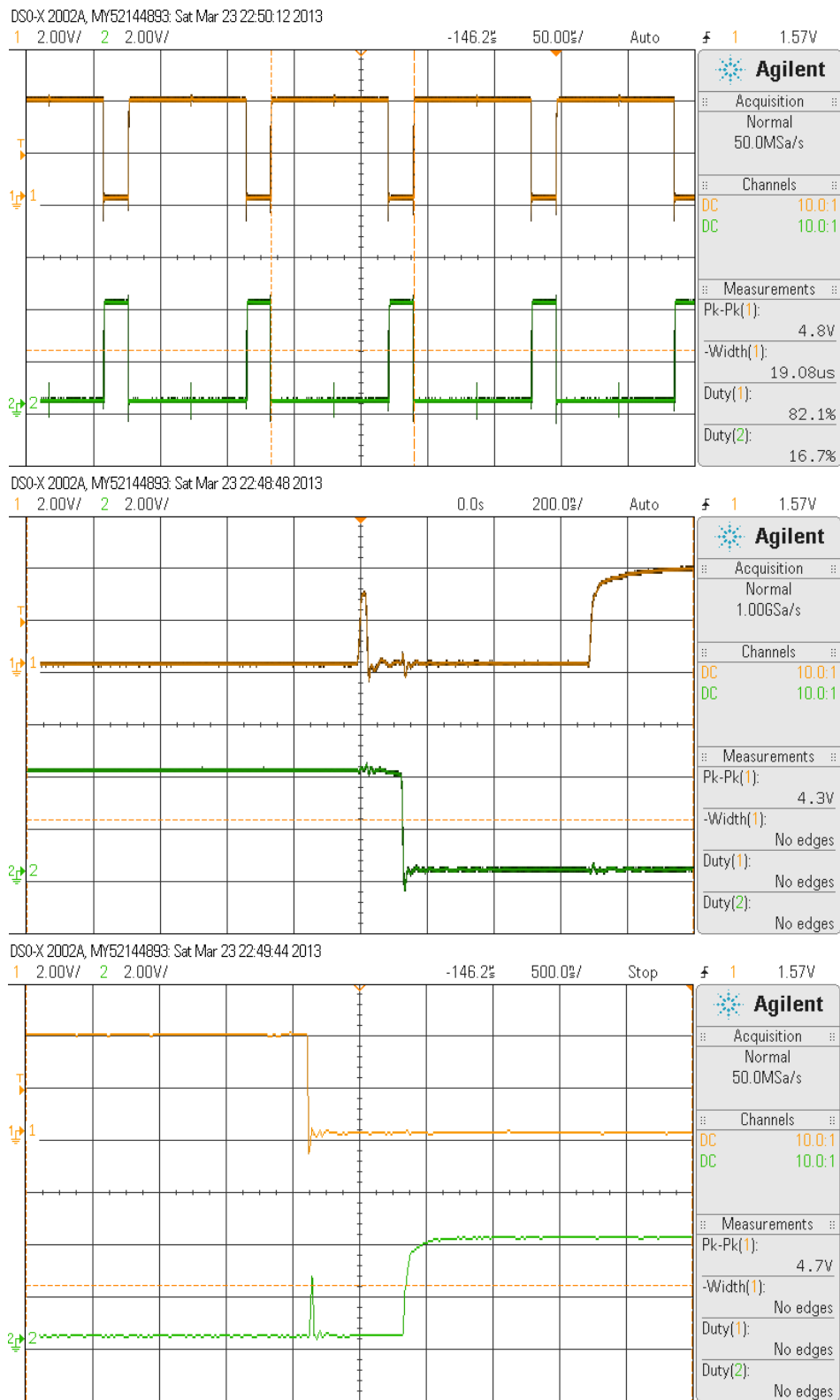


Figure 4.10: Outputs from the Delay Circuitry

The first plot in 4.10 shows both the PWM signal after the delay circuitry. It can be seen that the duty cycles of both don't add up to 100, which should almost happen if there were no dead band. The second plot shows the rising edge of the first PWM and the falling edge of the inverted PWM and the dead band between them is 600ns. The third plot is of the other rising/falling edge with a similar dead band time.

In the earlier plots, we can see that whenever there's a switching in one wave, there's a spike that occurs in the other. This can be dangerous and switch the wrong device ON. To eliminate them, we use a low pass RC filter with  $1k\Omega$  and  $0.1\mu F$  and it removes the spikes considerably. The results are shown in Fig: 4.11

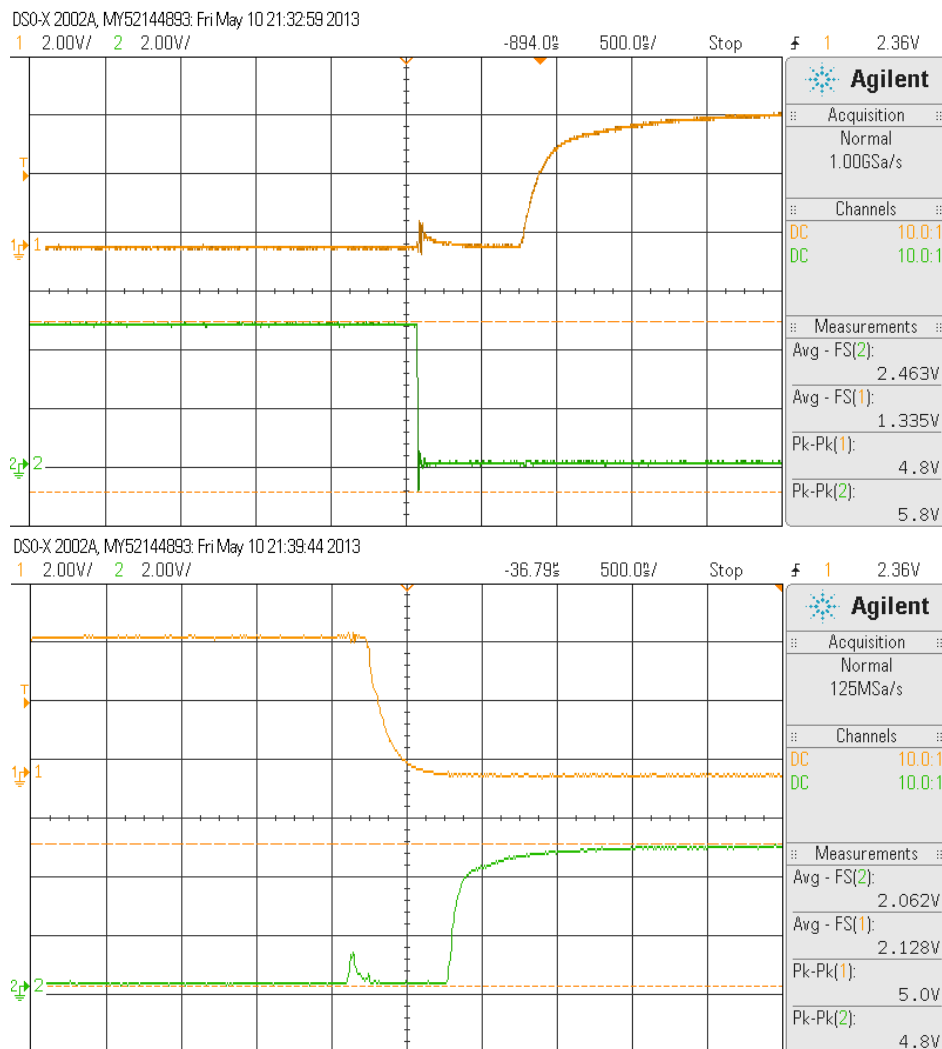


Figure 4.11: Outputs from the delay circuitry after correction



### 4.3 PI Controller Block

The PI controller has the comparator (for the reference value and the feedback value), the proportional and integral components and the adder for the P and I parts. It is also provided with zener diodes for protection of the circuit. The Op-amp IC LM318 is used to realize all the components and it is shown below. The comparator gives the error signal between the reference and the feedback and this is sent to the proportional and the integral terms separately before being added up in the adder. This is the essence of the PI block.

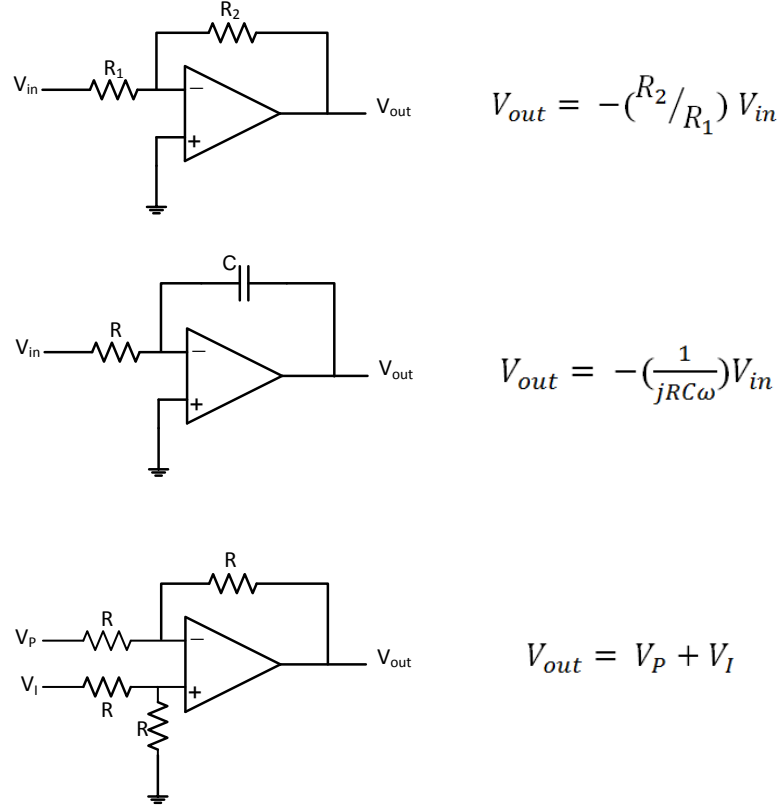


Figure 4.12: Proportional, Integral and Adder Components through Op-amps

The values of the resistors and the capacitors used will depend on the  $K_I$  and  $K_P$  values arrived at in the second chapter. So, here, the values of  $R$  and  $C$  are given to get the needed gains are calculated to be  $R_2 = R = 10k\Omega$ ,  $R_1 = 1k\Omega$  and  $C = 3.3nF$ . The entire PI block is diagrammatically shown in Fig 4.13. The zener diode is for protection and to avoid large voltages to go to the drive circuit.

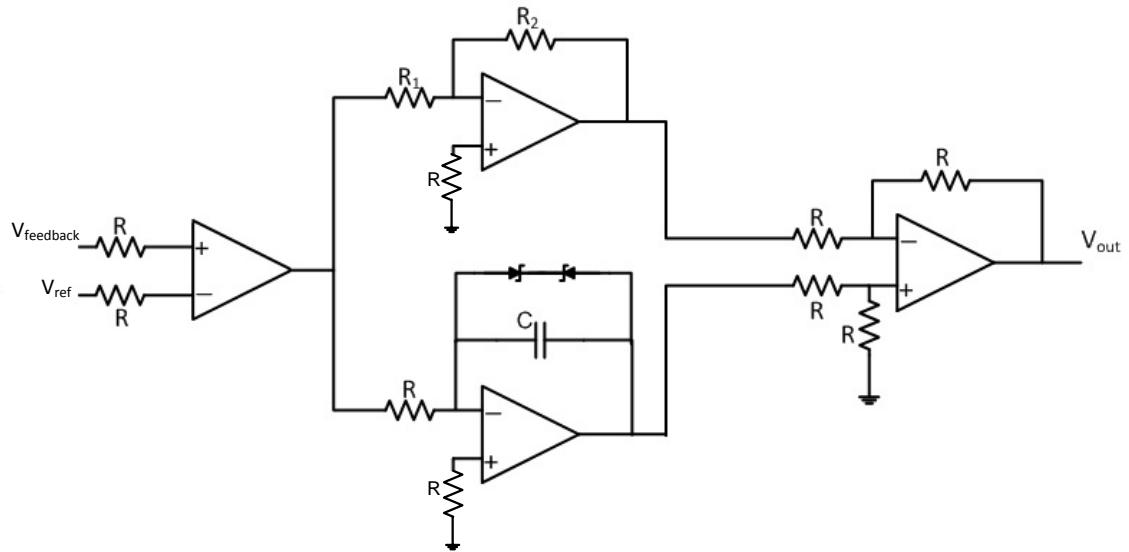


Figure 4.13: Complete PI controller block

## 4.4 Feedback Path and Current Transducer

Now, with the entire open loop in place, we need to just close the loop by giving current feedback to the PI-block to compare it with the reference value. To read off the current we use a current transducer and an op-amp to sufficiently amplify it to the right current value.

### Current Transducer LA-55P

We use LA-55P current transducer to read the current. It is rated at 50A, so it is well above the rated 20A and can be used in this. When it is used with a measuring resistance of  $220\Omega$  and used with armature current of the motor, we get voltages that can be used as feedback. When the calibration was done, the results were as in table 4.1 and plotted in fig 4.14.

This implies that the voltage read is directly proportional to the current in the motor and it has to be multiplied by a constant 3.1456 to reflect the real value of the current. For this, a simple op-amp is used. The output of this op-amp is given to the comparator in the PI block as a feedback, hence closing the loop.

Table 4.1: Calibration of the current transducer

| Armature Current(A) | Transducer Voltage(V) |
|---------------------|-----------------------|
| 2.22                | 0.77                  |
| 3.15                | 1.08                  |
| 3.705               | 1.25                  |
| 4.27                | 1.43                  |
| 4.71                | 1.57                  |
| 5.62                | 1.87                  |
| 6.38                | 2.11                  |
| 7.3                 | 2.4                   |
| 7.9                 | 2.59                  |
| 8.6                 | 2.79                  |
| 9                   | 2.93                  |
| 9.48                | 3.09                  |
| 10.125              | 3.29                  |
| 10.55               | 3.43                  |
| 11.092              | 3.59                  |
| 11.72               | 3.79                  |
| 12.06               | 3.9                   |
| 12.65               | 4.1                   |
| 13.115              | 4.26                  |

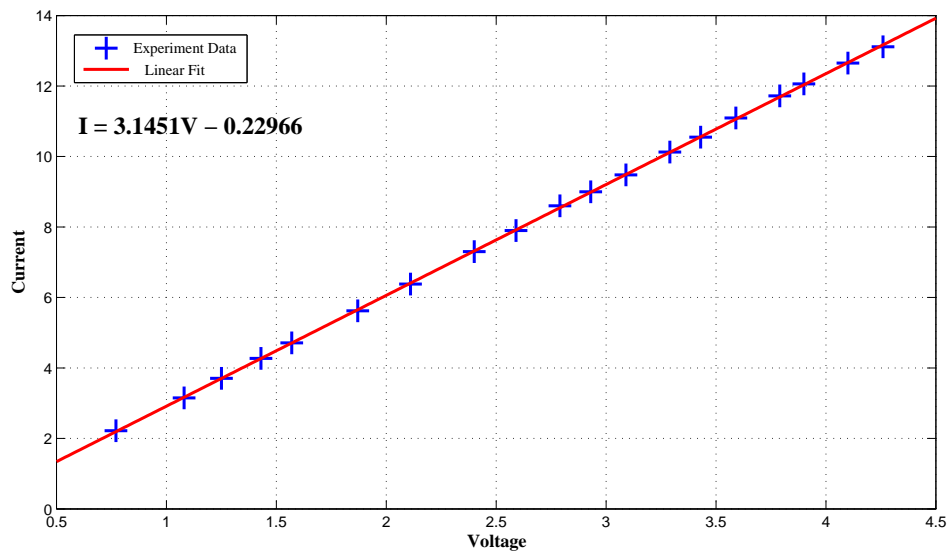


Figure 4.14: Plot of the transducer characteristics

## 4.5 Complete Circuit Diagram and Working

The complete circuit diagram of the current controller is shown here.

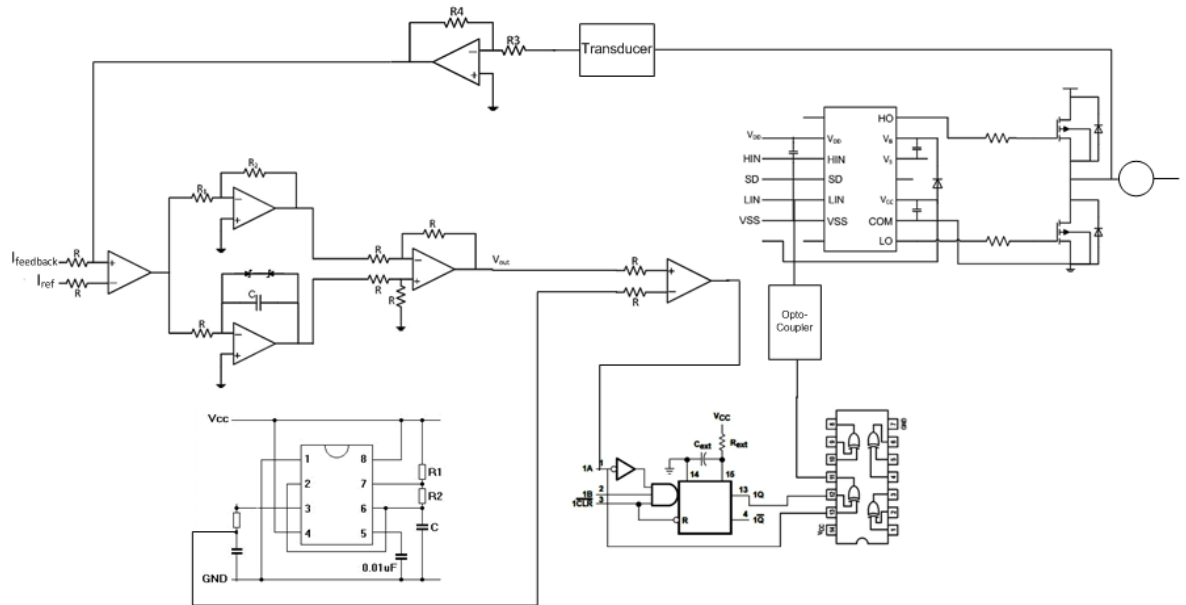


Figure 4.15: Complete Circuit Diagram

In brief, when the motor is switched on, the comparator 1 compares the reference current value with the feedback value (initially zero) and this is processed in the PI-controller and sufficiently amplified before being compared to the triangular carrier wave (from 555) in comparator 2. The resulting PWM is duplicated and inverted and a delay operation on these PWMs is done by X-ORing an impulse generated (from LS123) with the PWM itself. The two complementary signals with the dead band pass to the optocoupler and then to the IR2110 which drives both the MOSFETs in a leg based on the complementary PWMs. The armature current is read off from the motor by a transducer and fed back to the comparator 1 which subtracts this from the reference value and the error signal is processed again and this way, current settles at the reference value in its steady state with a small steady state error.

## 4.6 Testing and Results

The inverter board is tested on the high side and the low side separately on a rheostat load and the results of the high side are shown in the figure 4.16. In the first figure (high side on the first leg), the bottom trace is that of the input to the IR2110 IC while the top trace is that across the load. In the second figure (high side on the second leg) though, the bottom trace is the gate drive signal to the device and the top trace is across the load. There's a small ringing in both cases during the rising transition.

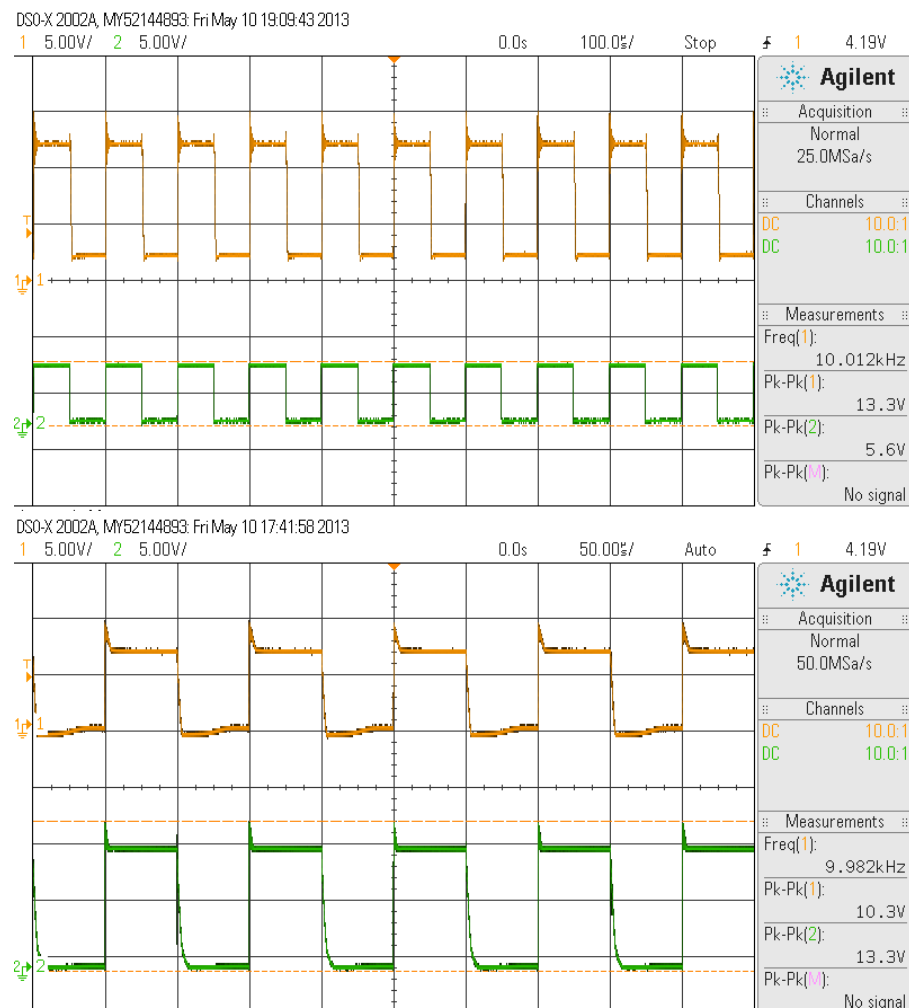


Figure 4.16: Results from the high-side devices

The next figure 4.17 is results from the low side devices on the board. Like before, the top figure is from the first leg low-side and the bottom one is from the second leg low-side. The top traces are those across the load and the bottom traces are from the gate drive and the optocoupler output respectively.



Figure 4.17: Results from the low-side devices

The PWM circuit is working well and given a DC signal, it is compared with the internal carrier triangular wave to get two complementary PWMa also having a dead band between them. The complementary duty cycle can be varied with the DC signal to the board between  $800mV$  and  $2.78V$ . The results are shown here in the figure 4.18.



Figure 4.18: Different duty cycles from the PWM and the dead band

The motor is run in open loop with the signals from the PWM circuit through the inverter board and the response is as found, when the duty cycle for the positive PWM is 80%. The supply voltage is 8.33V and 12.5.

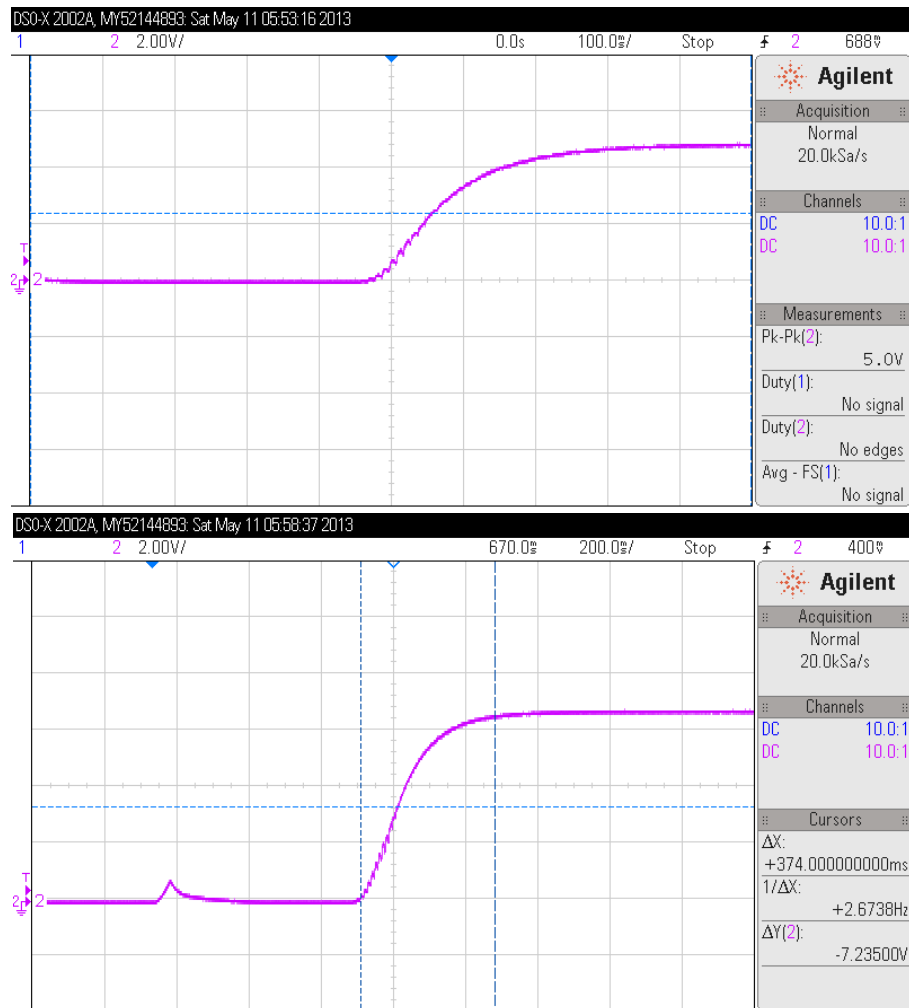


Figure 4.19: Open Loop Response of the Motor



# CHAPTER 5

## **Smmary and Conclusions**

In this project, an attempt was made to develop a current controller for a DC motor to be used in a tricycle. First, the model of the drive and the motor are arrived at, analytically. Secondly, the behavior of this model is simulated in a software simulink. Thirdly, the motor parameters are calculated through experiments and used in the simulink model of the second chapter. Lastly, the current controller is implemented in hardware in analog domain.

The hardware implementation is only partly successful because of the damage done to the inverter board during one of the tests. The blocks' individual functionality is tested and found to be working alright, but the closed loop testing using all the blocks was not possible due to afore mentioned reasons. In order to complete the project in the future, one has to redesign the inverter board to test the motor in closed loop.

# APPENDIX A

## DC Motor Transfer Function

The transfer function in the figure in section 2.3.3 is arrived at here. The first block diagram is that of a standard DC motor model and the required transfer function is derived sequentially here. The load is assumed to be proportional to speed.

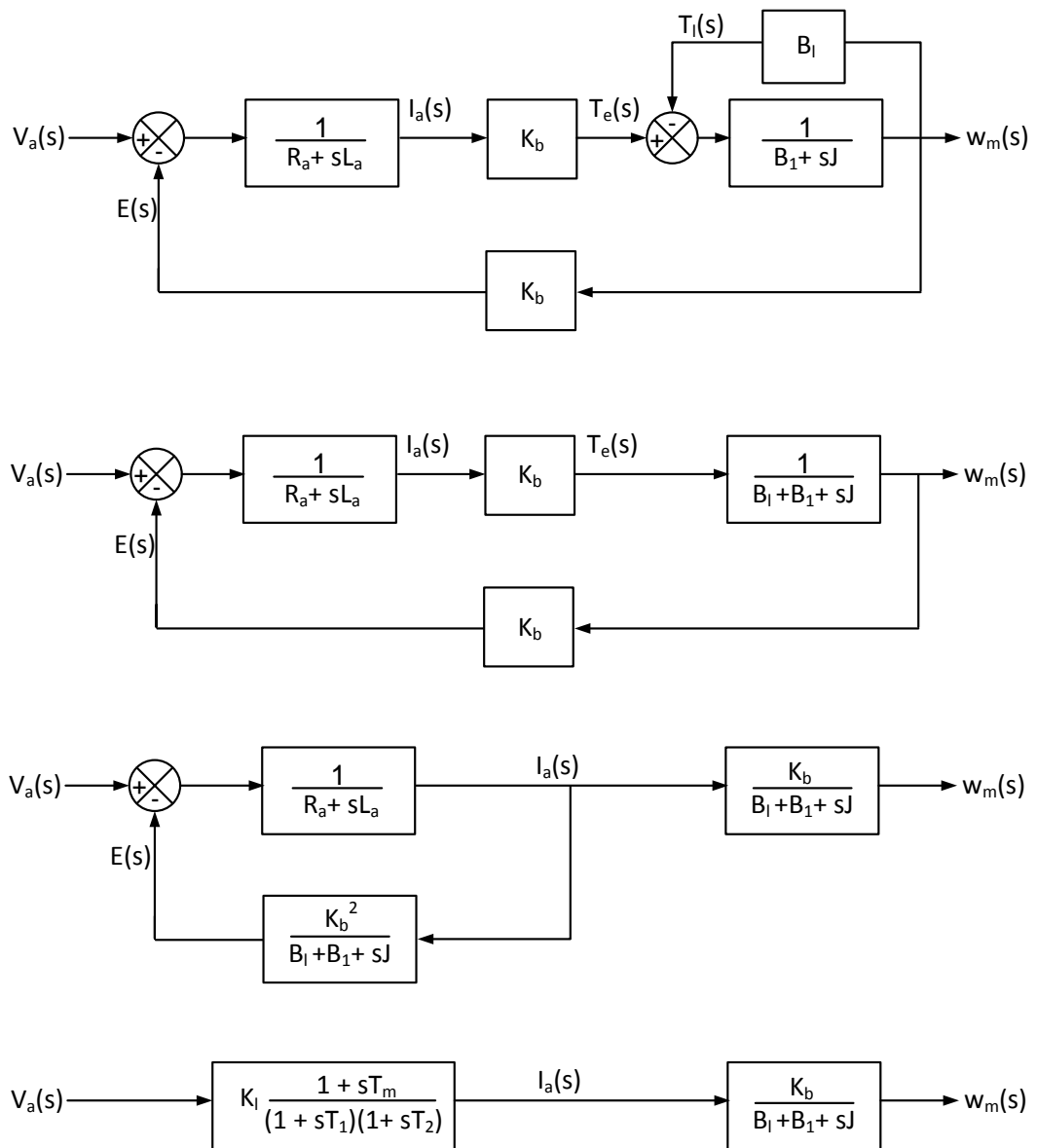


Figure A.1: DC motor transfer function

## REFERENCES

1. **Krishnan, R.**, *Electric motor drives: modeling, analysis, and control*. Prentice Hall, 2001.
2. **Vedam Subrahmanyam.**, *Power electronics*. J. Wiley, 1997.
3. **International rectifier**, (2007). Application Note AN-978. URL <http://www.irf.com/technical-info/appnotes/an-978.pdf>.
4. **555 Timer Circuits**, (2008). The Astable Multivibrator Circuit. URL <http://www.555-timer-circuits.com/astable-multivibrator.html>.
5. **Dr. Krishna Vasudevan, Prof .G. Sridhara Rao, Prof. P. Sasidhara Rao**. Electrical Machines-I. URL [http://nptel.iitm.ac.in/courses/IIT-MADRAS/Electrical\\_Machines\\_I/index.html](http://nptel.iitm.ac.in/courses/IIT-MADRAS/Electrical_Machines_I/index.html).